



CHORUS

This is the accepted manuscript made available via CHORUS. The article has been published as:

Gap scaling at Berezinskii-Kosterlitz-Thouless quantum critical points in one-dimensional Hubbard and Heisenberg models

M. Dalmonte, J. Carrasquilla, L. Taddia, E. Ercolessi, and M. Rigol

Phys. Rev. B **91**, 165136 — Published 29 April 2015

DOI: [10.1103/PhysRevB.91.165136](https://doi.org/10.1103/PhysRevB.91.165136)

Gap scaling at Berezinskii-Kosterlitz-Thouless quantum critical points in one-dimensional Hubbard and Heisenberg models

M. Dalmonte^{§,1,*} J. Carrasquilla^{§,2,†} L. Taddia^{§,3,‡} E. Ercolessi⁴ and M. Rigol⁵

¹*Institute for Quantum Optics and Quantum Information of the Austrian Academy of Sciences, and Institute for Theoretical Physics, University of Innsbruck, A-6020 Innsbruck, Austria*

²*Perimeter Institute for Theoretical Physics, Waterloo, Ontario, Canada N2L 2Y5*

³*Scuola Normale Superiore, Piazza dei Cavalieri 7, 56126 Pisa, Italy,*

and CNR-INO, UOS di Firenze LENS, Via Carrara 1, 50019 Sesto Fiorentino, Italy[§]

⁴*Dipartimento di Fisica e Astronomia, Università di Bologna and INFN, via Irnerio 46, 40127 Bologna, Italy*

⁵*Department of Physics, The Pennsylvania State University, University Park, PA 16802, USA*

(Dated: April 16, 2015)

We discuss how to locate critical points in the Berezinskii-Kosterlitz-Thouless (BKT) universality class by means of gap-scaling analyses. While accurately determining such points using gap extrapolation procedures is usually challenging and inaccurate due to the exponentially small value of the gap in the vicinity of the critical point, we show that a generic gap-scaling analysis, including the effects of logarithmic corrections, provides very accurate estimates of BKT transition points in a variety of spin and fermionic models. As a first example, we show how the scaling procedure, combined with density-matrix-renormalization-group simulations, performs extremely well in a non-integrable spin-3/2 XXZ model, which is known to exhibit strong finite-size effects. We then analyze the extended Hubbard model, whose BKT transition has been debated, finding results that are consistent with previous studies based on the scaling of the Luttinger-liquid parameter. Finally, we investigate an anisotropic extended Hubbard model, for which we present the first estimates of the BKT transition line based on large-scale density-matrix-renormalization-group simulations. Our work demonstrates how gap-scaling analyses can help to locate accurately and efficiently BKT critical points, without relying on model-dependent scaling assumptions.

PACS numbers: 05.70.Jk, 75.10.Pq, 71.10.Fd, 71.10.Pm

I. INTRODUCTION

Quantum phase transitions in one-dimensional (1D) systems are one of the most remarkable consequences of the enhanced role of quantum fluctuations in reduced dimensions.^{1–3} While systems with discrete symmetries, such as the Ising model, can still undergo phase transitions associated with the spontaneous breaking of those symmetries, 1D systems with continuous symmetries, such as spin-rotation or particle-number conservation, cannot get spontaneously broken under rather general conditions due to the Mermin-Wagner-Hohenberg theorem.^{4,5} Similarly to classical two-dimensional systems at finite temperature, 1D quantum systems endowed with continuous symmetries can still undergo a quantum phase transition according to the Berezinskii-Kosterlitz-Thouless (BKT) mechanism.^{6,7} Such transitions play a key role in the physics of 1D spin, bosonic, and fermionic models, which find incarnations as diverse as different magnetic compounds,^{3,8} and ultracold atom and molecule gases trapped in optical lattices.^{3,9–11}

In the BKT scenario, the phase transition point is conformal, and in its vicinity the gap closes exponentially as a function of the microscopic parameters.¹² This feature makes numerical investigations of BKT transitions challenging, as very large systems sizes are required in order to avoid severe finite-size effects. Usually, techniques from field theory can be used to pin down the transition point. These include methods that use correlation

functions to track the scaling dimension of relevant operators close to transition point,^{1,13,14} or entanglement entropies to monitor the behavior of the central charge of the system.^{15,16} While these approaches have provided notable insights in the context of several lattice models, it is highly desirable to develop and benchmark alternative methods based on the spectral properties, which do not rely on any *a priori* knowledge of the underlying field theory, and at the same time can cope well with logarithmic corrections. Moreover, gap-based methods are, from the computational side, potentially less demanding than evaluating correlations functions, and precise bounds on the error can be given when employing variational techniques such as the density-matrix-renormalization-group (DMRG).^{17–19}

Here, we show how refined gap-scaling analyses provide accurate insights on phase diagrams of 1D spin and fermionic models undergoing a BKT transition. Our technique relies on a recently proposed scaling ansatz for the gap close to the critical point, which was successfully applied to the t - V - V' model of spinless fermions in 1D (equivalent to the spin-1/2 XXZ chain with next-nearest neighbor $S^z S^z$ interactions)²⁰ and the 1D Bose-Hubbard model.²¹ All our calculations are done using DMRG, which allows us to accurately and efficiently determine the gaps needed for the scaling analyses.

As a first step in our study, in Sec. II, we apply the scaling approach to an $S = 3/2$ XXZ chain, where the exact location of the BKT point is known, but it is difficult

to pinpoint numerically owing to strong finite-size corrections. Using simulations with both periodic and open boundary conditions, we show that the scaling method is able to locate the transition point with errors at the $\sim 1\%$ level in the presence of strong logarithmic corrections (for periodic boundary conditions). In Sec. III, we discuss the feasibility of our approach for extended Hubbard models including nearest-neighbor interactions, where the existence and location of a BKT transition separating a spin-density-wave and a bond-ordered phase has been extensively debated.^{22–31} In Sec. IV, we investigate an anisotropic version of the EHM, the anisotropic-extended-Hubbard model, where spin-rotation symmetry is explicitly broken. For the latter model, we complement the gap scaling analysis with a correlation-function method based on the scaling of the Luttinger parameter, which provides an independent way to locate the transition point. Finally, we recapitulate the main results and discuss possible extensions of our work in Sec. V.

II. SPIN-3/2 XXZ CHAIN

Spin chains are prototypical models of one-dimensional (1D) quantum systems.³ The first spin chains introduced were of the Heisenberg (also known as XXX) type:³²

$$\hat{H} = J \sum_j \vec{S}_j \cdot \vec{S}_{j+1}, \quad (1)$$

where $J \in \mathbb{R}$ and \vec{S} are matrices belonging to some finite-dimensional representation of $SU(2)$. In the antiferromagnetic case, $J > 0$, and for general finite-dimensional representations of $SU(2)$, Haldane^{33–35} conjectured that the ground state should be gapped for integer values of S and gapless (belonging to the $SU(2)_1$ Wess-Zumino-Novikov-Witten universality class) for half-integer values of S . This conjecture has been extensively verified analytically and numerically (see, e.g., Refs. 36–38).

The XXZ chain, on the other hand, is a generalization of the Heisenberg one that is obtained by introducing anisotropy along one, namely the z -, axis. The Hamiltonian can be cast in the form

$$\hat{H} = -J \sum_j (S_j^x S_{j+1}^x + S_j^y S_{j+1}^y - J_z S_j^z S_{j+1}^z), \quad (2)$$

where J_z is the anisotropy coefficient (we set $J = 1$ as our energy unit in what follows). For half-integer S , $J_z = 1$ is a critical point separating a conformal phase (a Tomonaga-Luttinger liquid, $-1 < J_z < 1$) from a Néel phase ($J_z > 1$)^{38–40}. This phase transition is known to belong to the BKT universality class, and, in the vicinity of the critical point, the low-energy spectrum is well-described by a sine-Gordon model:^{1,2,41}

$$\hat{H} = \int dx \left\{ \frac{v_s}{2\pi} \left[\frac{(\partial_x \vartheta)^2}{K} + K(\partial_x \varphi)^2 \right] + g \cos[\sqrt{4\pi} \varphi] \right\},$$

where v_s is the sound velocity, ϑ and φ are conjugated density and phase bosonic fields, K is the Luttinger-liquid parameter, related to the compactification radius $R_\vartheta = 1/R_\varphi$ of the fields via $K = 1/(4\pi R_\vartheta^2)$,² and the last term gives rise to a finite mass in the spectrum for $K < 1/2$.

While for the $S = 1/2$ integrable case numerical methods work relatively well locating $J_z = 1$ as the transition point,^{2,42} strong logarithmic corrections arise for $S \geq 3/2$, making the numerical detection of the BKT point difficult.⁴³ In certain cases precise knowledge of the underlying logarithmic scaling of K in terms of perturbed conformal field theories can be provided, making methods based on correlation-function applicable.^{38,44} As the latter rely on *ad hoc* assumptions based on the symmetry content of the theory at the critical point, they cannot, in general, be extended to other models.

It is our aim in the following to investigate how gap scaling methods, which do not rely on field theoretical assumptions, can be employed to locate BKT transition points. In this context, the $S = 3/2$ XXZ model represents an ideal benchmark, since, on the one hand, the location of the transition point is known, and, on the other hand, strong logarithmic corrections need to be incorporated, providing a strict test for the reliability of the method itself. This scaling analysis used here was applied to the $S = 1/2$ integrable case in Ref. 20, and the critical point was found to be at $J_z^c = 1.01 \pm 0.005$, in agreement with the exact result.

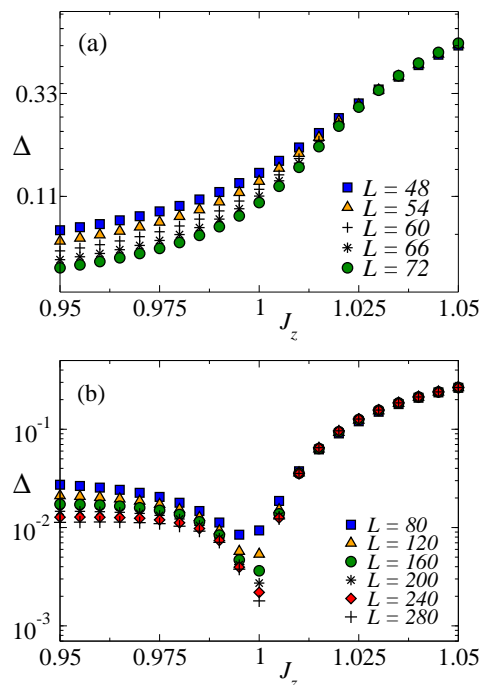


FIG. 1. (Color online) Energy gaps for the spin-3/2 XXZ chain with PBCs (a) and OBCs (b), as a function of J_z and for different values of L . In both cases, the gap axis has a logarithmic scale for sake of clarity.

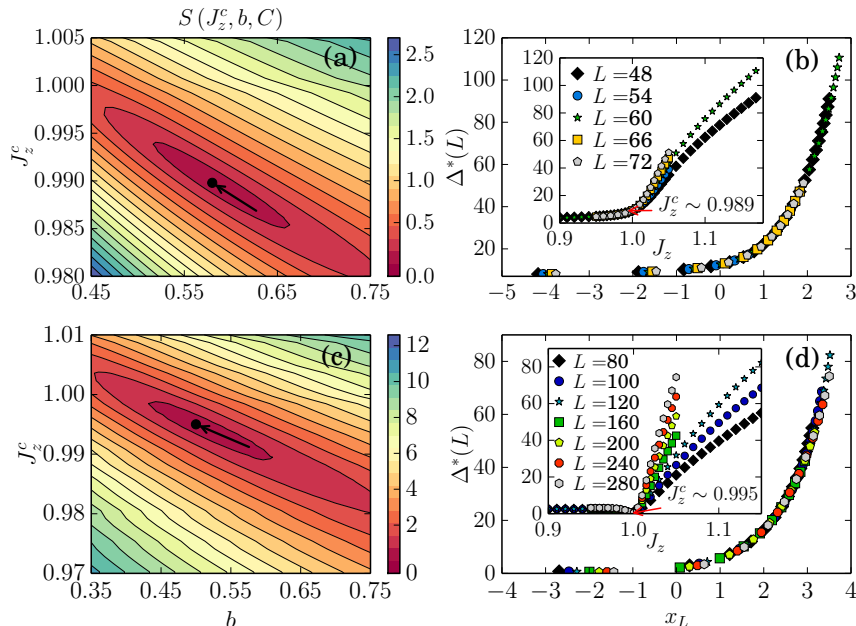


FIG. 2. (Color online) (a) Contour plot of the sum of squared residuals $S(J_z^c, b, C)$ for the XXZ model with PBCs. The arrow signals the location of the minimum value of S . The black lines are equally spaced contour lines where S is constant. (b) Best collapse of the data for $\Delta^*(L)$ vs x_L corresponding to $J_z^c = 0.989$, $b = 0.58$, and $C = -4.5$. The inset shows the rescaled gap vs J_z . A similar analysis for the system with OBCs is presented in panels (c) and (d). J_z and $\Delta^*(L)$ are presented in units of J , while b and S are shown in units of $J^{1/2}$ and J^2 , respectively.

Following Refs. 20 and 21, we locate the critical point of the BKT transition in the $S = 3/2$ case by studying the scaling of the spin excitation gap $\Delta(L) = E_0(L) - E_1(L)$ on finite systems, where $E_p(L)$ is the ground state energy at size L in the magnetization sector $\sum_j S_j^z = p$. We have performed DMRG simulations both with periodic (PBCs) and open (OBCs) boundary conditions: in the former (latter) case, we consider system sizes in the range $L \in [48, 72]$ ($[60, 280]$), keeping up to $m = 1200$ (768) Schmidt states in the finite-size sweeping procedure. We have performed 6 (4) finite-size sweeps and achieved a truncation error less, in all cases, than 10^{-5} (10^{-8}). The typical errors in the gap are of order 2×10^{-4} (10^{-6}) for PBCs (OBCs). By comparing the results for different boundary conditions, we gain insights on the effects of translational invariance, which is broken under OBCs. In both cases, we consider anisotropies in the range $J_z \in [0.95, 1.05]$. In Figs. 1(a) and 1(b), we plot the energy gap $\Delta(L)$ as a function of J_z , for different system sizes L , and for PBCs and OBCs, respectively. In the chains with PBCs [Fig. 1(a)], the gap exhibits a rather smooth behavior with changing J_z and increasing L . For OBCs [Fig. 1(b)], a dip occurs very close to the critical point. As expected, under both boundary conditions, the magnitude of the gap decreases as L increases for $J_z < 1$.

The method described in Ref. 20 and 21 is based on the following ansatz for the scaling of the gap in the vicinity

of the phase transition,

$$L\Delta(L) \times \left(1 + \frac{1}{2 \ln L + C}\right) = F\left(\frac{\xi}{L}\right), \quad (3)$$

where F is a scaling function, C is a nonuniversal constant to be determined, and ξ is the correlation length. This scaling ansatz is an attempt to include known logarithmic corrections to the gap in a BKT transition⁴⁵ and reduces to the analog relation for the resistance (which also vanishes exponentially) in the charge-unbinding transition of the two-dimensional classical Coulomb gas at the critical point.⁴⁶ In the latter case, the universal nature of the coefficient in front of $\ln(L)$ can be traced back to the logarithmic corrections of the Weber-Minnhagen finite-size scaling relation of the dielectric function, which is, in turn, related to the superfluid stiffness (see Refs. 46 and 47). For isotropic chains, conformal field theory calculations show that the prefactor in front of the logarithm is universal and equals 2.^{44,48,49} Note that in a BKT transition, the correlation length diverges as $\xi \sim \Delta^{-1} \sim \exp(b/\sqrt{J_z - J_z^c})$, where b is independent of J_z . Because of the divergence of the correlation length at the critical point, the function $F(\xi/L)$ becomes system-size independent, and thus the data for the rescaled gap $\Delta^*(L) \equiv L\Delta(L) [1 + 1/(2 \ln L + C)]$ for different system sizes L will be independent of L for $J_z \leq J_z^c$. Additionally, plots of $\Delta^*(L)$ vs ξ/L should collapse onto a unique curve representing F . In order to plot the scaling collapse, one can rewrite the relation in

Eq. (3) by taking the logarithm of the argument of F and considering an alternative function f with argument $x_L = \ln L - \ln \xi$.

We determine the critical point by adjusting the parameters J_z^c , b , and C such that the best collapse of the curves $\Delta^*(L)$ vs x_L is obtained. To do that, we represent f through an arbitrary high-degree polynomial and fit it on a dense grid of values of J_z^c , b , and C , to the calculated values of $\Delta^*(L)$ and x_L . The desired parameters J_z^c , b , and C are selected by minimizing the sum of squared residuals $S(J_z^c, b, C)$ of the fit. We ensure that the results are robust to the choice of polynomial and the interval of values of J_z used in the fits.

The results of this procedure applied to the data in Fig. 1 are summarized in Fig. 2. In Fig. 2(a), we present a density plot corresponding to $S(J_z^c, b, C)$ for the XXZ model with PBCs, which exhibits a clear minimum at $J_z^c = 0.989 \pm 0.01$, $b = 0.58 \pm 0.04$, and $C = -4.5 \pm 0.2$. In Fig. 2(b), we display $\Delta^*(L)$ vs x_L for the given set of parameters that minimize $S(J_z^c, b, C)$. The data clearly collapses onto a unique curve representing the function f . The sensitivity of the results to the selection of the interval of values of J_z used in the fit is also included in the error bars such that our results are independent of its choice. In the inset, the curves for the rescaled gap vs J_z and different system sizes merge around the critical value J_z^c found through the minimization procedure. This indicates that the ansatz in Eq. (3) describes well the numerical data around the critical point.

In Fig. 2(c), we present $S(J_z^c, b, C)$ for the XXZ model with OBCs, which exhibits a minimum at $J_z^c = 0.995 \pm 0.004$, $b = 0.50 \pm 0.02$. In this case, the values of C that minimize S are arbitrarily large; in practice this means that logarithmic corrections to the gap are suppressed when OBCs are used. In Fig. 2(d), we show $\Delta^*(L)$ vs x_L for the given set of parameters that minimize $S(J_z^c, b, C)$. As in the case with PBCs, the data is seen to collapse to a unique curve. In this case, it is also verified that the curves of the rescaled gap vs J_z merge around the critical point retrieved from the minimization procedure.

Our results for the critical anisotropy coefficient J_z^c , both for OBCs and PBCs, are very close to the analytical result, indicating that the data and critical behavior of the gap are well described by Eq. (3). The use of OBCs has clear advantages. First, from the DMRG perspective, the use of OBCs generally allows simulating larger system sizes while keeping lower errors in the energy gaps: for the same accuracy obtained keeping m states and OBCs, one requires of the order of m^2 states in the case of PBCs. Second, for the present model, the logarithmic corrections are suppressed when OBCs are used, thus effectively reducing the number of parameters that need to be determined in the minimization of S . While the precise reason for this suppression is not known, we note that the same behavior in the Bose-Hubbard model²¹. We speculate that, for those models, certain marginal operator contribute vanishes at the transition point, akin to what happens at the BKT point of the Majumdar-Ghosh

chain.⁵⁰

III. ONE-DIMENSIONAL EXTENDED HUBBARD MODEL

We now extend our analysis of the gap-scaling method to multicomponent models, where the interplay between different energy scales can make the pinning down of BKT transitions even more complex than in single-species models. The first example we consider is the 1D extended Hubbard model (EHM), defined by the Hamiltonian:

$$\hat{H} = -t \sum_{j,\sigma} \left(\hat{c}_{j,\sigma}^\dagger \hat{c}_{j+1,\sigma} + \text{H.c.} \right) + U \sum_j \hat{n}_{j,\uparrow} \hat{n}_{j,\downarrow} + V \sum_j \hat{n}_j \hat{n}_{j+1}, \quad (4)$$

where $\hat{c}_{j,\sigma}$ (with $\sigma = \uparrow, \downarrow$) is a spin-1/2 fermionic annihilation operator, $\hat{c}_{j,\sigma}^\dagger$ is its creation counterpart, and $\hat{n}_j = \sum_\sigma \hat{n}_{j,\sigma}$, with $\hat{n}_{j,\sigma} = \hat{c}_{j,\sigma}^\dagger \hat{c}_{j,\sigma}$, is the site occupation operator; t is the hopping amplitude ($t = 1$ sets our energy scale in what follows), U is the on-site interaction coefficient, and V parametrizes nearest-neighbor interactions. The phase diagram of this model has recently attracted quite some interest^{22–30} due to the presence of a spontaneously dimerized phase supporting bond [or, more precisely, bond-charge-density-wave (BCDW)] order in the vicinity of the $U = 2V$ line, with $U, V > 0$. The BCDW phase intervenes between a charge-density-wave (CDW) and a spin-density-wave (SDW) phase, present, respectively, when $V \gg U$ and $U \gg V$. While, across this line, the low-energy charge sector of the theory remains always gapped, the spin sector undergoes a BKT transition between SDW and BCDW at a critical value of V . This critical point has been debated, in particular, to discern whether a BCDW phase exists and, if it does, in which parameter regime.

Here, we apply the gap-scaling analysis to the spin gap at $U = 4$ in order to detect the SDW to BCDW

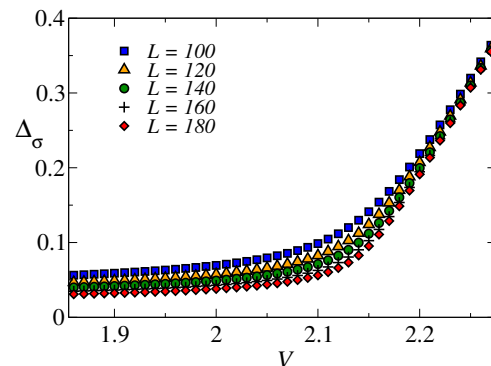


FIG. 3. (Color online) Spin gaps for the EHM as functions of V for different values of L , with $U = 4$ and OBCs.

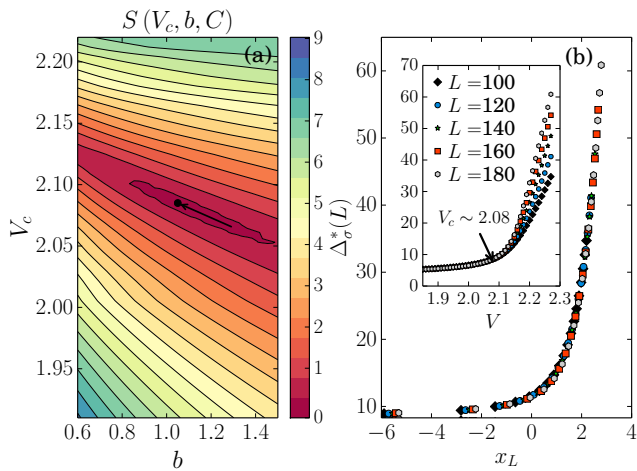


FIG. 4. (Color online) (a) Contour plot of the sum of squared residuals $S(V_c, b, C)$ for the EHM model with OBCs. (b) Best collapse of the data for $\Delta_\sigma^*(L)$ vs x_L corresponding to $V_c = 2.08$, $b = 1.05$, and $C = -31$. The inset shows the rescaled gap vs V .

phase transition. The subsequent BCDW-CDW transition point is located around $V = 2.16$.²⁴ The best estimates for the BKT between SDW and BCDW phases based on the finite-size scaling of the Luttinger parameter (under the assumption that logarithmic corrections are negligible) and on entanglement witnesses predict $V^{\text{BKT}} \simeq 1.88 - 2.02$.^{13,24,30,51} We have performed DMRG simulations with chains up to $L = 180$ sites (with OBCs), keeping up to 1024 states and up to 8 finite-size sweeps in order to get truncation errors of order 10^{-7} (and a corresponding error in the spin gap of order 10^{-5}). In Fig. 3, we plot our results for the spin gap Δ_σ as a function of V , where $\Delta_\sigma(L) = E_{L,0}(L) - E_{L,1}(L)$, with $E_{p,q}(L)$ is the ground state energy at size L for a system with p particles and magnetization q . For the smallest values of V reported in the plot, Δ_σ decreases with increasing system size, while it does not seem to change with system size for the largest values of V reported. This suggests that the spin gap closes at some V_c in the thermodynamic limit, but does not quite help locating that point.

In Fig. 4, we summarize the results obtained through the gap-scaling procedure based on the data in Fig. 3. The minimum of the function $S(V_c, b, C)$, displayed in Fig. 4(a), is located at $V_c = 2.08 \pm 0.02$, $b = 1.05 \pm 0.04$, and $C = -31 \pm 1$. The data produces the collapse presented in Fig. 4(b) and the inset shows that the data merge around $V \sim 2.08$, in agreement with the critical value obtained from the minimization procedure.⁵² We note that our critical strength V_c is above the estimates in Refs. 13 and 24, which means that a reduction of the size of the BCDW region is observed, in agreement with Ref. 30. Nevertheless, our estimate is still consistent with the presence of an intervening BCDW state in the phase diagram. We conclude that the gap scaling analysis, combined with numerical results on smaller chain sizes with

respect to the ones employed in correlation-function and entanglement-witness studies, still provides a rather accurate figure of merit for the phase transition point at a one-percent level.

IV. ONE-DIMENSIONAL ANISOTROPIC EXTENDED HUBBARD MODEL

A simple variant of the EHM is its anisotropic version, the so called anisotropic extended Hubbard model (AEHM)⁵³

$$\begin{aligned} \hat{H} = & -t \sum_{j,\sigma} \left(c_{j,\sigma}^\dagger c_{j+1,\sigma} + \text{H.c.} \right) + U \sum_j \hat{n}_{j,\uparrow} \hat{n}_{j,\downarrow} + \\ & + V(1 - \delta) \sum_{j,\sigma} \hat{n}_{j,\sigma} \hat{n}_{j+1,\sigma} + \\ & + V(1 + \delta) \sum_j \left(\hat{n}_{j,\uparrow} \hat{n}_{j+1,\downarrow} + \hat{n}_{j,\downarrow} \hat{n}_{j+1,\uparrow} \right), \end{aligned} \quad (5)$$

whose main difference with respect to Eq. (4) is in the last two terms, which reduce the original $SU(2)$ spin symmetry to $U(1)$, for any $\delta \neq 0$. We again set the hopping amplitude $t = 1$ as our energy scale, and focus on the $\delta = 0.2$ case. The phase diagram of this model has been explored by combining exact-diagonalization ($L \leq 14$) and level-spectroscopy techniques⁵⁴, and supports a finite bond-spin-density-wave (BSDW) for $U \lesssim 3$, intervening between a SDW and a CDW for $U \gg V$ and $V \gg U$, respectively, as in the EHM.^{53,55}

Here, we are interested in the BKT transition separating the BSDW and the CDW for both $U = 1.5$ and $U = 2.5$. We determine the transition points by means of DMRG simulations of much larger system sizes than those accessible to exact diagonalization calculations.⁵³ For the gap analysis, we have performed DMRG simulations in lattices with up to $L = 200$ sites, keeping up to 512 states and up to 8 finite-size sweeps in order to get truncation errors of order 5×10^{-7} (and a corresponding error in the gap of order 10^{-5}). The results are illustrated in Fig. 5. In addition, we have evaluated the transition point by a complementary technique based on correlation functions that we describe below.

In Fig. 6, we report the results of our scaling analysis based on the data in Fig. 5. The minimum of the function $S(V_c, b, C)$, displayed in Fig. 6(a), is located at $V_c = 0.82 \pm 0.03$, $b = 3.2 \pm 0.1$, and $C = -18.8 \pm 0.2$. The data produces the collapse presented in Fig. 6(b) and its inset shows a region around $V \sim 0.82$ where the data merge, as expected from Eq. (3). The same procedure applied to $\delta = 0.2$ and $U = 2.5$ yields $V_c = 1.14 \pm 0.02$, $b = 7.0 \pm 0.5$, and $C = -49 \pm 0.5$. These critical parameters are in agreement with the phase diagram from level spectroscopy measurements presented in Refs. 53 and 55. However, our estimates are extracted from much larger system size data, and result more accurate.

A. Transition point from the spin Luttinger parameter

In order to have a quantitative benchmark for the gap-scaling analysis for this model, we have investigated the location of the BKT transition between BSDW and CDW using correlation-functions methods based on the underlying field-theoretical structure.⁵³ At the transition point, the spin Luttinger parameter flows to the BKT separatrix, that is, $K_S^* = 1$. In finite size samples, it is possible to extract $K_S(L)$ by monitoring the behavior of the spin structure factor:

$$S_s(k) = \frac{1}{L} \sum_{j,\ell} e^{ik(j-\ell)} (\langle S_j^z S_\ell^z \rangle - \langle S_j^z \rangle \langle S_\ell^z \rangle), \quad (6)$$

with $S_j^z = (\hat{n}_{j,\uparrow} - \hat{n}_{j,\downarrow})/2$, and applying the relation:¹

$$K_S(L) = L \frac{S_s(2\pi/L)}{2}, \quad (7)$$

which stems from the low-momentum behavior of the structure factor in a gapless phase, $S_s(q) \simeq qK_S/\pi$.⁵⁶ For each system size, taking the smallest numerically available $q = 2\pi/L$, this leads to Eq. (7). In order to avoid edge effects, we have performed DMRG simulations on samples with anti-periodic-boundary conditions⁵⁷ for various system sizes up to $L = 48$, using up to 10 finite-size sweeps and 1800 states per block. The truncation and energy error were kept smaller than 10^{-5} (5×10^{-5}) for $L \leq 40$ ($L > 40$). Single-site expectation values (such as $\langle \hat{n}_{j,\sigma} \rangle$) were found to be translationally invariant up to 10^{-7} corrections at most. Results for $K_S(V)$ vs V for different system sizes are reported in Fig. 7(a).

For each system size, we fit the function $K_S(V)$ with a fourth-order polynomial, and determine the value of $V_0(L)$ such that $K_S(L; V_0) = 1$ [point at which the curves for $K_S(V)$ vs V cross the dashed line in Fig. 7(a)]. A finite-size-scaling analysis is then carried out on $V_0(L)$ in order to extract the critical value of V in the thermodynamic limit by assuming the scaling form

$$V_0(L) = V_c + a_0 L^{-a_1}, \quad (8)$$

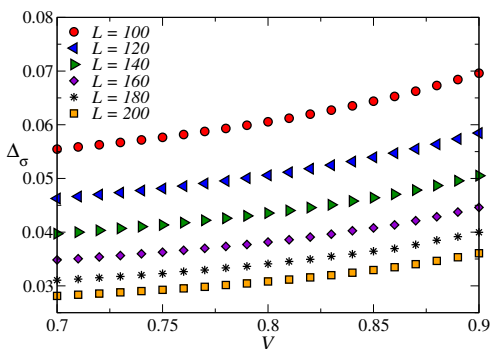


FIG. 5. (Color online) Spin gaps for the AEHM as functions of V for different values of L , $\delta = 0.2$, $U = 1.5$, and OBCs.

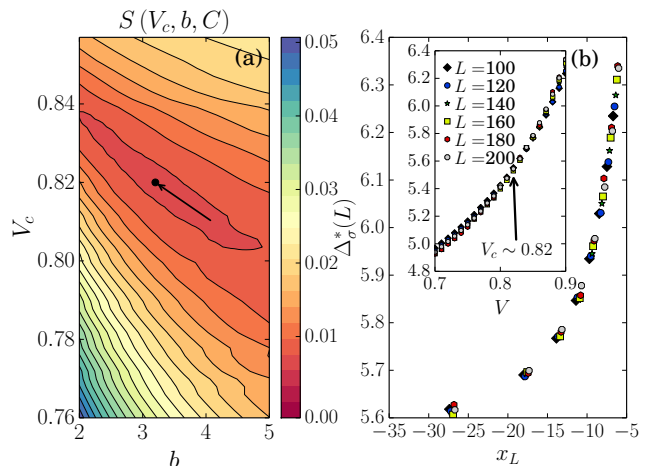


FIG. 6. (Color online) (a) Contour plot of the sum of squared residuals $S(V_c, b, C)$ for the AEHM model with OBCs, $U = 1.5$ and $\delta = 0.2$. (b) Best collapse of the data for $\Delta_\sigma^*(L)$ vs x_L corresponding to $V_c = 0.82$, $b = 3.2$, and $C = -18.8$. The inset shows the rescaled gap vs V .

and performing a fourth-order polynomial fit using both least-square and Nelder-Mead methods. In addition, we have performed a linear fit using sizes $L > 20$ for comparison. The results are illustrated in Fig. 7(b). For $U = 1.5$, we find that $V_c = 0.81 \pm 0.04$, where the error is estimated by comparing the fitting procedure using different sets of system sizes and different fitting techniques.

The critical point for $U = 1.5$ obtained using the Luttinger-liquid parameter is consistent with the one from the gap-scaling analysis. However, the accuracy achieved in the latter is far superior to that of the former approach. This is understandable since the Luttinger-liquid-based approach involves: (i) a fit and an extrapolation, and (ii) smaller system sizes, because of the need to compute correlations avoiding boundary effects, than those available in the gap scaling analysis. Furthermore, the gap scaling analysis accounts for logarithmic corrections [see Eq. (3)], which are difficult to incorporate in the scaling of the Luttinger parameter.

V. CONCLUSIONS AND OUTLOOK

We have studied various BKT transitions by means of a recently introduced gap-scaling analysis. Starting with the spin-3/2 XXZ model, where the critical anisotropy is known to be $J_z = 1$, we ascertained the validity of the gap scaling procedure. Using both PBCs and OBCs, we found excellent agreement between the numerical results and the analytical one. We have shown that the scaling ansatz in Eq. (3) describes well the critical behavior of the gap data on finite systems, as observed from the quality of the data collapses presented in Figs. 2, 4, and 6. For the first time, we have successfully applied

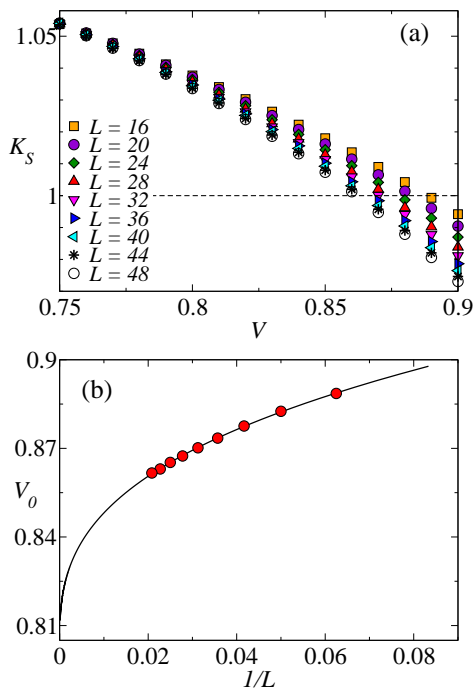


FIG. 7. (Color online) (a) Spin Luttinger parameter as a function of V for different system sizes for the AEHM. The dashed line, $K_S = 1$, depicts the value of K_S at the critical point. (b) Scaling of the value of V at which $K_S = 1$ for each system size vs $1/L$. All results reported are for $U = 1.5$ and $\delta = 0.2$.

the gap scaling methodology to extended Hubbard models, where the interplay between different energy scales in the system can make the determination of critical parameters much more difficult than in spin models. In both the EHM and AEHM, our results are consistent with, but in principle more accurate (as they systematically include logarithmic corrections) than, previous estimates obtained using other techniques. We should stress that the critical parameters reported here for the transitions in the AEHM are the first to be obtained since early exact diagonalization results in small system sizes,^{53,55} which are usually affected by large finite-size effects. We have also compared our results from the gap scaling analysis with those from a method based on the determination of the Luttinger liquid parameter across the transition. They were found to be in good agreement, but the gap scaling analysis is much more accurate.

We stress that the gap scaling analysis discussed here offers significant advantages over other methods to detect BKT transitions used in the literature. First, the scaling ansatz in Eq. (3) includes logarithmic corrections to the gap, which are generally significant in BKT

transitions.^{45,46} Second, this methodology can be indistinctly applied to transitions involving the closing of either a charge or a spin gap, i.e., one can equally well study problems involving spins, fermions, bosons, multicomponent systems, etc.. This constitutes an advantage over well established techniques such as level spectroscopy, which, e.g., are hardly applicable to bosonic models²¹ where the Hilbert space grows extremely fast as a number of components, preventing an accurate finite-size scaling analysis. Third, the gap is a quantity that, for large system sizes, can be obtained in different unbiased computational techniques, such as DMRG and quantum Monte Carlo approaches. Fourth, in DMRG (and usually in quantum Monte Carlo) simulations, the energies used in the determination of the gaps are variational, i.e., they are bounded and their quality can be easily assessed.

The demonstration of the aforementioned generality paves the way toward additional studies of models whose location of a BKT transition is still debated. With comparable computational resources as the ones employed here, one could investigate the so-called asymmetric Hubbard model,^{58,59} where a BKT transition has been predicted separating a two-channel LL phase and a SDW in the repulsive regime, but where numerical and analytical approaches predicted different transition point locations.^{58,60} Moreover, a computationally more demanding application could be the identification of different pairing regimes in three- and four-component Hubbard models. There, in the absence of $SU(N)$ symmetries, a rich pairing pattern has been numerically and analytically put forward.⁶¹ However, a precise estimate of the transition lines is challenging due to strong spin-charge mixing, and as such, the gap scaling method could potentially serve as an unbiased estimate for the transition between the different pairing regimes in case an exact BKT nature can be proven.

VI. ACKNOWLEDGMENTS

We thank C. Degli Esposti Boschi and F. Ortolani for help with the DMRG code. M.D. was supported by the ERC Synergy Grant UQUAM, SIQS, and SFB FoQuS (FWF Project No. F4006-N16). J.C. acknowledges support from the John Templeton Foundation. Research at Perimeter Institute is supported through Industry Canada and by the Province of Ontario through the Ministry of Research & Innovation. L.T. acknowledges financial support from the EU integrated project SIQS. E.E. acknowledges the INFN grant QUANTUM for partial financial support. M.R. was supported by the National Science Foundation, Grant No. PHY13-18303.

* marcello.dalmonte@uibk.ac.at

† jcarrasquilla@perimeterinstitute.ca

- [‡] luca.taddia2@gmail.com
- [§] These authors contributed equally to this work.
- ¹ T. Giamarchi, *Quantum Physics in One Dimension* (Oxford University Press, 2003).
 - ² A. O. Gogolin, A. A. Nersisyan, and A. M. Tsvelik, *Bosonization and Strongly Correlated Systems* (Cambridge University Press, 2004).
 - ³ M. A. Cazalilla, R. Citro, T. Giamarchi, E. Orignac, and M. Rigol, *Rev. Mod. Phys.* **83**, 1405 (2011).
 - ⁴ N. D. Mermin and H. Wagner, *Phys. Rev. Lett.* **17**, 1133 (1966).
 - ⁵ P. C. Hohenberg, *Phys. Rev.* **158**, 383 (1967).
 - ⁶ V. L. Berezinskii, *Sov. Phys. JETP* **34**, 610 (1972).
 - ⁷ J. M. Kosterlitz and D. J. Thouless, *J. Phys. C* **6**, 1181 (1973).
 - ⁸ T. Giamarchi, *Int. J. Mod. Phys. B* **26** (2012).
 - ⁹ I. Bloch, J. Dalibard, and W. Zwerger, *Rev. Mod. Phys.* **80**, 885 (2008).
 - ¹⁰ Z. Hadzibabic, P. Krüger, M. Cheneau, B. Battelier, and J. Dalibard, *Nature* **441**, 1118 (2006).
 - ¹¹ E. Haller, R. Hart, M. J. Mark, J. G. Danzl, L. Reichsöllner, M. Gustavsson, M. Dalmonte, G. Pupillo, and H.-C. Nagerl, *Nature* **466**, 597 (2010).
 - ¹² C. Itzykson and J.-M. Drouffe, *Statistical Field Theory* (Cambridge University Press, 1989).
 - ¹³ A. W. Sandvik, L. Balents, and D. K. Campbell, *Phys. Rev. Lett.* **92**, 236401 (2004).
 - ¹⁴ S. Rachel, N. Laflorencie, H. F. Song, and K. L. Hur, *Phys. Rev. Lett.* **108**, 116401 (2012).
 - ¹⁵ P. Calabrese and J. Cardy, *Journal of Statistical Mechanics: Theory and Experiment* **2004**, P06002 (2004).
 - ¹⁶ A. Laeuchli and C. Kollath, *J. Stat. Mech.*, P05018 (2008), 0803.2947.
 - ¹⁷ S. R. White, *Phys. Rev. Lett.* **69**, 2863 (1992).
 - ¹⁸ S. R. White, *Phys. Rev. B* **48**, 10345 (1993).
 - ¹⁹ U. Schollwöck, *Rev. Mod. Phys.* **77**, 259 (2005).
 - ²⁰ T. Mishra, J. Carrasquilla, and M. Rigol, *Phys. Rev. B* **84**, 115135 (2011).
 - ²¹ J. Carrasquilla, S. R. Manmana, and M. Rigol, *Phys. Rev. A* **87**, 043606 (2013).
 - ²² Y. Z. Zhang, *Phys. Rev. Lett.* **92**, 246404 (2004).
 - ²³ M. Ménard and C. Bourbonnais, *Phys. Rev. B* **83**, 075111 (2011).
 - ²⁴ S. Ejima and S. Nishimoto, *Phys. Rev. Lett.* **99**, 216403 (2007).
 - ²⁵ M. Tsuchiizu and A. Furusaki, *Phys. Rev. B* **69**, 035103 (2004).
 - ²⁶ K.-M. Tam, S.-W. Tsai, and D. Campbell, *Phys. Rev. Lett.* **96**, 036408 (2006).
 - ²⁷ M. Nakamura, *Phys. Rev. B* **61**, 16377 (2000).
 - ²⁸ E. Jeckelmann, *Phys. Rev. Lett.* **89**, 236401 (2002).
 - ²⁹ L. Barbiero, A. Montorsi, and M. Roncaglia, *Phys. Rev. B* **88**, 035109 (2013).
 - ³⁰ S. Glocke, A. Klümper, and J. Sirker, *Phys. Rev. B* **76**, 155121 (2007).
 - ³¹ P. Sengupta, A. Sandvik, and D. Campbell, *Physical Review B* **65**, 155113 (2002).
 - ³² W. Heisenberg, *Zeitschrift für Physik* **49**, 619 (1928).
 - ³³ F. D. M. Haldane, *Bull. Am. Phys. Soc.* **27**, 181 (1982).
 - ³⁴ F. Haldane, *Physics Letters A* **93**, 464 (1983).
 - ³⁵ F. D. M. Haldane, *Phys. Rev. Lett.* **50**, 1153 (1983).
 - ³⁶ I. Affleck and E. Lieb, *Letters in Mathematical Physics* **12**, 57 (1986).
 - ³⁷ I. Affleck, T. Kennedy, E. H. Lieb, and H. Tasaki, *Phys. Rev. Lett.* **59**, 799 (1987).
 - ³⁸ K. Hallberg, X. Q. G. Wang, P. Horsch, and A. Moreo, *Phys. Rev. Lett.* **76**, 4955 (1996).
 - ³⁹ H. J. Schulz, *Phys. Rev. B* **34**, 6372 (1986).
 - ⁴⁰ I. Affleck and F. Haldane, *Phys. Rev. B* **36**, 5291 (1987).
 - ⁴¹ F. D. M. Haldane, *Phys. Rev. Lett.* **47**, 1840 (1981).
 - ⁴² M. Dalmonte, E. Ercolessi, and L. Taddia, *Phys. Rev. B* **84**, 085110 (2011).
 - ⁴³ M. Dalmonte, E. Ercolessi, and L. Taddia, *Phys. Rev. B* **85**, 165112 (2012).
 - ⁴⁴ I. Affleck, D. Gepner, H. J. Schulz, and T. Ziman, *Journal of Physics A: Mathematical and General* **22**, 511 (1989).
 - ⁴⁵ F. Woynarovich and H. P. Eckle, *Journal of Physics A: Mathematical and General* **20**, L443 (1987).
 - ⁴⁶ M. Wallin and H. Weber, *Phys. Rev. B* **51**, 6163 (1995).
 - ⁴⁷ H. Weber and P. Minnhagen, *Phys. Rev. B* **37**, 5986 (1988).
 - ⁴⁸ K. Nomura and A. Kitazawa, *cond-mat/0201072*.
 - ⁴⁹ J. L. Cardy, *Journal of Physics A: Mathematical and General* **19**, L1093 (1986).
 - ⁵⁰ S. Eggert, *Phys. Rev. B* **54**, 9612 (R) (1996).
 - ⁵¹ C. Mund, O. Legeza, and R. Noack, *Phys. Rev. B* **79**, 245130 (2009).
 - ⁵² We have also checked that using the scaling ansatz proposed in Ref. 27 gives results compatible with the present one at the 1% level.
 - ⁵³ H. Otsuka, *Phys. Rev. Lett.* **84**, 5572 (2000).
 - ⁵⁴ K. Nomura and K. Okamoto, *J. Phys. A* **27**, 5773 (1994).
 - ⁵⁵ H. Otsuka, *Phys. Rev. B* **63**, 125111 (2001).
 - ⁵⁶ R. Clay, A. Sandvik, and D. Campbell, *Phys. Rev. B* **59**, 4665 (1999).
 - ⁵⁷ For $L = 4n, n \in \mathbb{N}$, we observe stronger finite-size effects for comparable system sizes, possibly due to the fact that the SDW phase becomes frustrated.
 - ⁵⁸ M. A. Cazalilla, A. Ho, and T. Giamarchi, *Phys. Rev. Lett.* **95**, 226402 (2005).
 - ⁵⁹ L. Barbiero, M. Casadei, M. Dalmonte, C. D. E. Boschi, E. Ercolessi, and F. Ortolani, *Phys. Rev. B* **81**, 224512 (2010).
 - ⁶⁰ T. Roscilde, C. Degli Esposti Boschi, and M. Dalmonte, *Europhysics Letters* **97**, 23002 (2012).
 - ⁶¹ S. Capponi, G. Roux, P. Lecheminant, P. Azaria, E. Boulat, and S. R. White, *Phys. Rev. A* **77**, 013624 (2008).